A Platinum Open Access Journal for Organic Chemistry

Paper

Free to Authors and Readers

DOAJ Seal

Arkivoc **2026** (2) 202612577

High-throughput evaluation of potential commercial photocatalysts: investigation of Sudan Black B

Anna Porcher, Marine Le Stum, Jean-Christophe Cintrat, and Eugénie Romero*

Université Paris-Saclay, CEA, INRAE, Département Médicaments et Technologies pour la Santé (DMTS), SCBM, 91191 Gif-sur-Yvette, France

Email: eugenie.romero@cea.fr

Received 03-11-2026 **Accepted** 09-03-2026 **Published on line** 09-09-2026

Abstract

The development of affordable and sustainable organic photocatalysts remains a key challenge in visible-light photoredox catalysis. Through high-throughput screening of commercially available dyes, Sudan Black B was identified as a promising candidate. Optical studies revealed strong visible-light absorption, solvatochromism, and photoinduced structural changes under UV and blue irradiation. Photocatalytic evaluation showed that SBB promotes oxidative transformations via a Type I reactive oxygen species pathway, with higher reactivity under purple light. Although its efficiency does not compete benchmark catalysts, this work demonstrates for the first time that a Sudan dye can operate as a photocatalyst and validates a high-throughput strategy for identifying accessible organic dyes for sustainable photoredox applications.

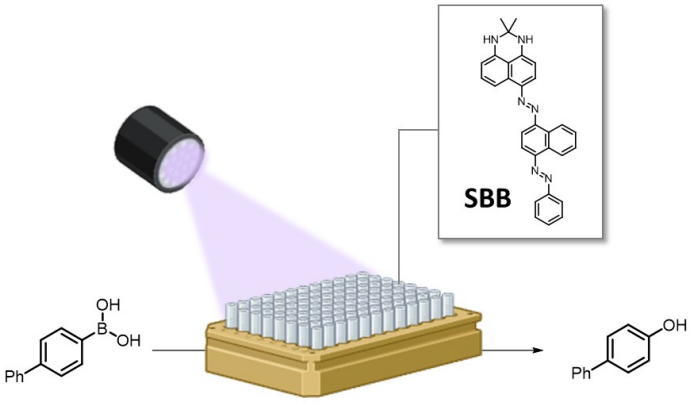

High-Throughput screening of photocatalyst

Keywords: High-Throughput Screening, organic dye, photosensitizer, reactive oxygen species

 ©AUTHOR(S)

Introduction

Visible light photoredox chemistry has emerged as one of the most important fields in organic synthesis the last two decades, allowing transformations previously unachievable under thermal conditions.[1-7] Light-mediated redox catalysis appears as an essential tool as it can allow radical generation under controlled and mild conditions. Photoredox catalysis has changed the way we think about molecule construction, in academic and industrial ecosystems.[6,7] Ruthenium and iridium-based metal complexes have shown impressive efficiency in many transformations, thanks to a wide range of redox potentials, tuned via the polypyridyl ligands variation.[10-15] Among the few utilized organic photocatalysts (PC) capable of competing if not surpassing metal complexes' efficiency, we can mention 4CzIPN, largely adopted by the community and utilized in industrial processes.[16] Practically, UV/Visible light is commonly used as the source of light to generate the PC in its excited state. Depending on the redox properties of the PC, a single electron transfer then occurs, allowing the formation of the substrate of interest.

However, the low abundance of metals, or their toxicity, forced the scientific community to explore metal-free solutions. In that context, the use of light-mediated catalysis by organophotocatalysts resonates with the current ecological and economic challenges the world is facing with regard to the problems caused by metal extractions, including human rights or environmental consequences. Despite the few structures of organophotocatalysts widely utilized in academia as industry,[17-19] the need for cheap, stable, and easily accessible organic photocatalysts is still ongoing to cover the redox potentials necessary to investigate the chemical space of photoredox catalysis. That said, the necessary time for the development of such an efficient photocatalyst, but even more the required time to make it popular in academic or industrial ecosystems are tremendous, time we don't have to face our current environmental and economic, and social problems.

We have focused our interest on existing organic dyes, and evaluated the photoredox efficiency of a library of 16 known organic dyes on 3 different transformations of interest. Among hits, one photocatalyst bearing a chemical structure from the family of Sudan dyes has been highlighted. Sudan dyes are aromatic compounds containing azo group. These organic dyes are easily accessible on the market, and find applications in a wide range of applications. Sudan Red dyes found applications in the food industry for decades. Most of the Sudan dyes are used to color hydrocarbon solvents, oils, fats, waxes, shoes, and floor polishes.[20-22] Some Sudan dyes find specific applications in histology, hematology, or diagnostic assays as it is well known and used to stain phospholipids and intracellular lipids.[23,24] As far as we know, no investigation of their potential as PCs in organic synthesis has been reported. With in mind the aim of identifying new already accessible organic PCs, we have identified Sudan Black B (SBB) shown in the Figure 1 as a potential interesting organic dye for photoredox applications. SBB has been primarily used in histology and cytology to stain lipids, phospholipids, and lipoproteins in tissues and cells, appearing as a dark blue or black stain. It is widely applied for detecting fat droplets in frozen tissue sections, visualizing myelin in nerve tissue, and distinguishing granulocytes in blood smears particularly in diagnosing acute myeloid leukemia.[25] In microbiology, it helps identify lipid inclusions like poly-β-hydroxybutyrate in bacteria, and in forensic science, it is used to detect latent fingerprints on oily or greasy surfaces. Its strong affinity for lipids and oxidative byproducts makes it valuable in both diagnostic and research settings. However, to the best of our knowledge, the potential of SBB for photochemical applications has never been investigated.

 ©AUTHOR(S)

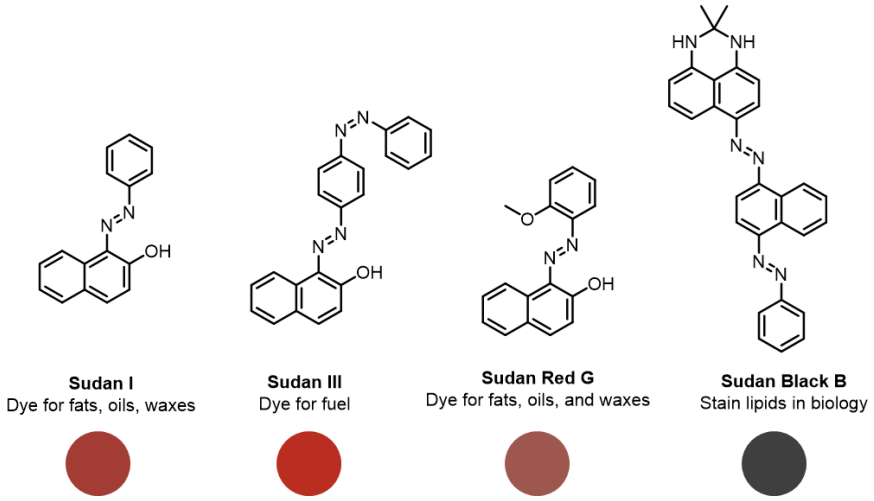

Figure 1. Examples of chemical structures of Sudan dyes with associated color of the powder form: Sudan I, III, Red G and Black B.

In this paper, we describe the investigation of the optical properties of SBB as well as its ability to photocatalyze chemical transformations.

Results and Discussion

With in mind the identification of organic dyes as new organic PCs, we have focused our interest on existing organic dyes, known as fluorescent probes or dyes for microscopy for instance, and evaluated the photoredox efficiency of a library of 16 known organic dyes (among which SBB, azulene, disperse dyes, resazurin, black eryochrom T or toluidine blue) on 4 different transformations of interest (see SI for organic dyes structures and transformations of interest). To do so, we have employed the High-Throughput Experimentation technology to miniaturize and parallelize reactions in a 96 well plate format, working at 10 micromole scale.[26-31] This technology was originally used to accelerate the optimization of reaction by screening reaction conditions. Its initial use was repurposed here for the benefit of the high-throughput screening of potential photocatalysts. Among hits, Sudan Black B, also known as black Cerol, has been highlighted as capable of promoting the oxidation of boronic acid (Figure 2). From this observation, we have decided to evaluate the optical properties of SBB, to understand its potential as organic PC.

 ©AUTHOR(S)

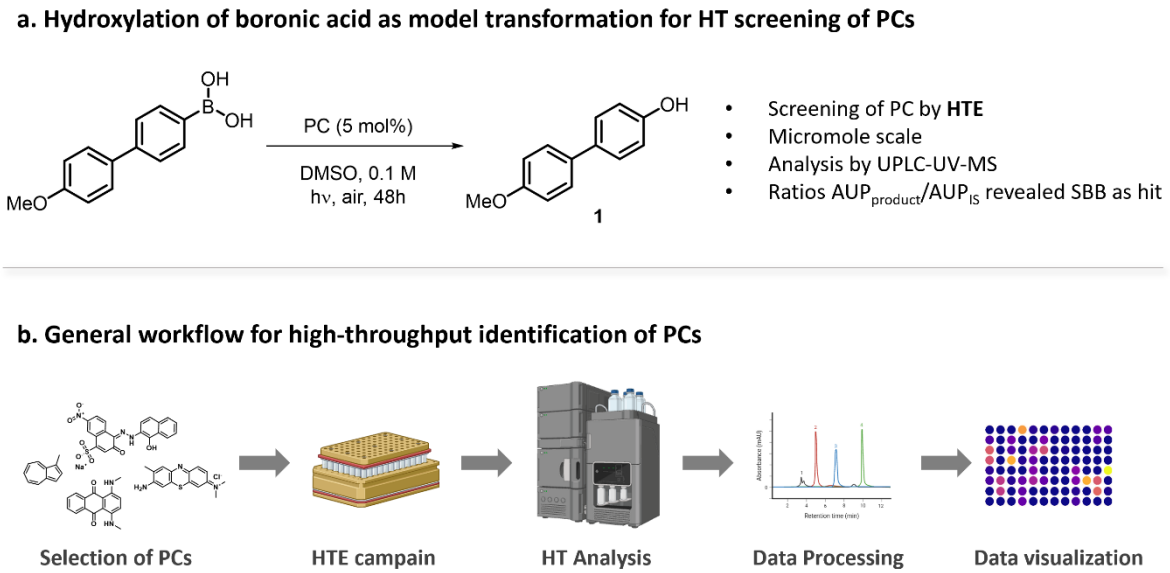

Figure 2. a. Hydroxylation of boronic acid as model transformation for screening of potential PCs; b. General workflow for high-throughput identification of new PCs.

In addition to the intrinsic properties of a photocatalyst, such as its electronic structure, redox potential, and stability, its cost is a critical factor influencing its widespread adoption, both in research and development and in industrial process chemistry. SBB is commercially available from many suppliers at a very low price (3.5€/g for SBB vs 236€/g for $Rubpy_3Cl_2$ or 965€/250mg for 4-CzIPN).

In order to be applied as PC in organic synthesis, it has to answer several property requisites. Indeed, a good photocatalyst for organic synthesis should possess several key properties to efficiently drive photochemical reactions. First, it must have an appropriate electronic structure, with a defined band gap or well-defined HOMO-LUMO gap, enabling it to absorb light effectively in the desired wavelength range. The excited-state properties of the catalyst are crucial, as the molecule should be capable of undergoing photoexcitation to generate reactive species, such as charge-separated states or excited-state radicals, which are essential for driving chemical transformations. The redox potential of the catalyst's excited states should be suitable for the desired electron transfer processes, facilitating oxidation or reduction of substrates, or affording effective energy transfer. Additionally, the photocatalyst must exhibit stability under the reaction conditions, including resistance to photodegradation and the ability to be regenerated after each catalytic cycle. Finally, selectivity is important, as the catalyst should promote the desired reaction pathway without leading to side reactions, often by controlling the electronic distribution in the excited state.

Optical properties. SBB is described in the literature with a maximum absorption in the red region (596–605 nm).[32] We have re-evaluated the absorption and emission spectra of SBB, measured in dimethylsulfoxide (DMSO), dichloromethane (DCM) and acetonitrile (MeCN).

 ©AUTHOR(S)

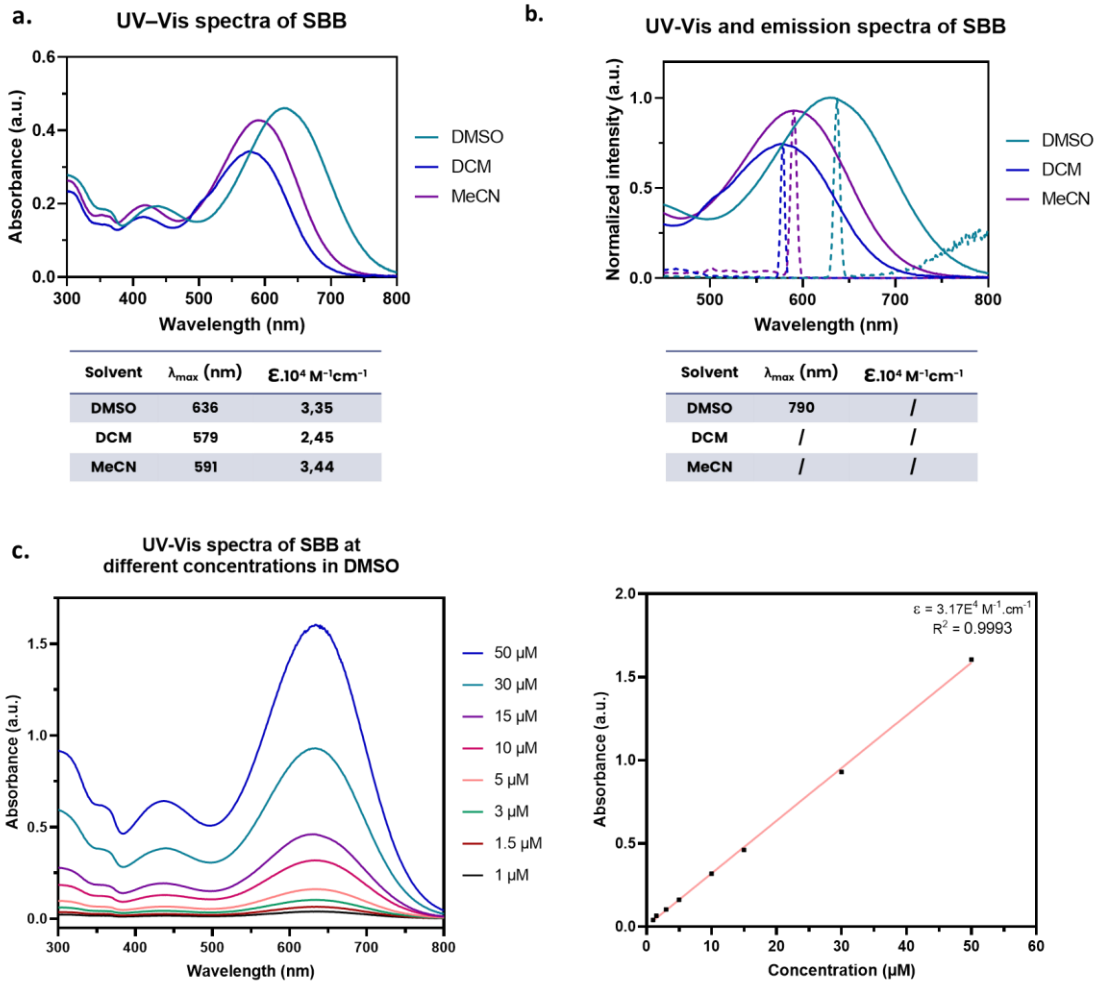

Solvent	λ_{max} (nm)	Ɛ.10⁴ M⁻¹cm⁻¹
DMSO	636	3,35
DCM	579	2,45
MeCN	591	3,44

Solvent	λ_{max} (nm)	Ɛ.10⁴ M⁻¹cm⁻¹
DMSO	790	/
DCM	/	/
MeCN	/	/

Figure 3. a. Absorption spectra of SBB in DMSO, DCM and MeCN at 10^{-5}M; b. Absorption and emission spectra of SBB in DMSO, DCM and MeCN at 10^{-5}M; c. Absorption spectra of SBB in DMSO at different concentrations.

SBB strongly absorbs in the UV and visible regions in DMSO (Figure 3a, light blue curve), with its primary absorption peak centered around 600–630 nm, but the spectrum extends from 500 nm to 700 nm. This broad absorption range suggests that SBB can absorb a significant portion of visible light, which is a good advantage for photochemical processes that rely on visible light. The dye's absorption in this range can be attributed to its π-π electronic transitions* within the azo group (-N=N-) and the aromatic rings. Despite its ability to absorb visible light, SBB exhibits low fluorescence, and its emission is observed in the 800 nm range in DMSO (Figure 3b, light blue curve). The low emission seems to indicate that SBB does not efficiently re-emit the absorbed energy. This weak fluorescence suggests that nonradiative decay mechanisms, such as internal conversion or internal relaxation, are predominant in its excited-state dynamics. However, its strong absorption, including in the low-energy irradiation range, may benefit photoinduced transformations such as reactions involving singlet oxygen generation.

We have also evaluated the photostability of the chemical structure of SBB in DMSO, which is photostable up to 48 h. The solvatochromic effect in a panel of organic solvents has also been investigated. A shift of 57 nm of the λ_{max} of the red-light absorbing band is observed when switching from DCM to DMSO (Figure 3a, pink curve). This observation is important in photocatalysis, as the light source has to be adjusted to maximize the

 ©AUTHOR(S)

potential of the PC. It is also worth mentioning that no emission is observed in DCM and MeCN (Figure 3b, pink and dark blue curves).

Then we decided to evaluate the photo-switching properties of SBB. Indeed, azo compounds are known for their photo-switching properties, which allow them to undergo reversible structural changes upon exposure to light. These compounds typically exist in two isomeric forms: a trans isomer (more stable) and a cis isomer (less stable), with the transition between these forms being triggered by light absorption. Upon irradiation with UV light, the azo compound often undergoes a trans-to-cis isomerization, changing its shape and sometimes its physical properties, such as solubility or color. Conversely, visible light or sometimes heat can induce the cis-to-trans reversion. This photo-switching behavior can be reversible, making azo compounds useful in a variety of applications, including molecular switches, photocatalysis, drug delivery systems, and smart materials. In the case of SBB, these photo-switching properties can be more difficult to evaluate as two azo groups are present in its chemical structure.

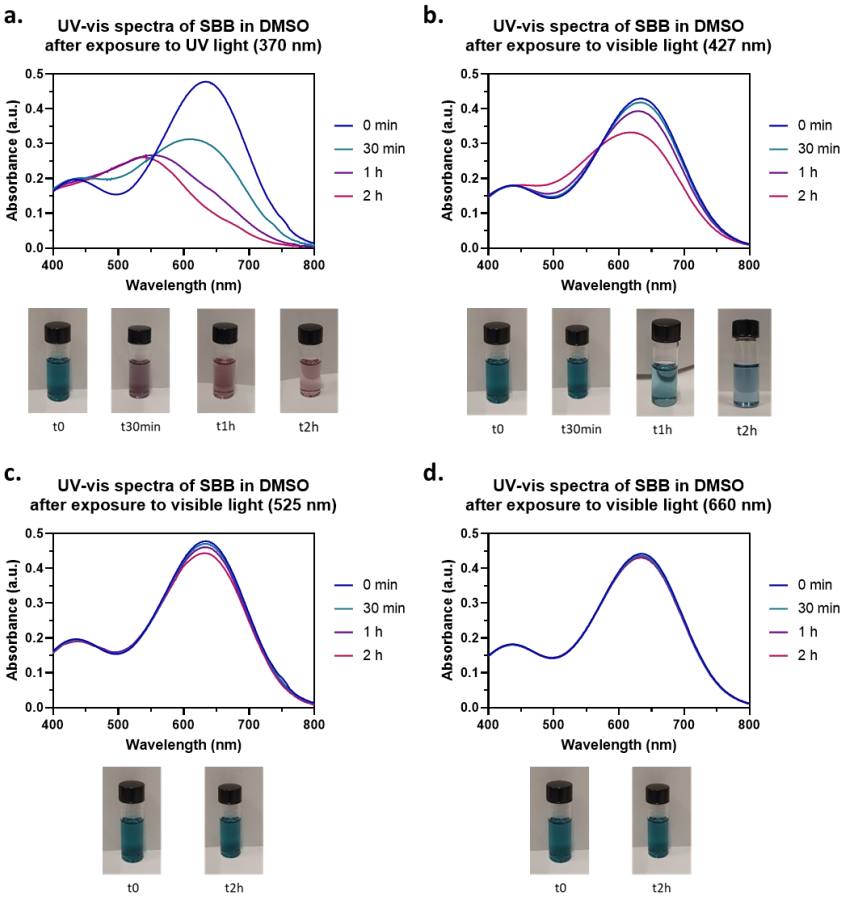

Figure 4. Photostability properties of SBB in DMSO at 10^{-5}M under different irradiation wavelengths.

We have evaluated the absorption of SBB over 2 h of irradiation, at 370 nm, 450 nm, 525 nm and 660 nm. While SBB absorbs intensely in the red region, irradiation at 525 or 660 nm does not affect the absorption spectrum over 2 h of irradiation. However, under UV and blue light, respectively 370 and 450 nm, the absorption spectrum is highly influenced. Indeed, under irradiation in DMSO, the absorption band at 650 nm disappears in favor of a new band centered at 550 nm. The color of the solution is also affected, and switches from a blue to a purple solution. These experiments seem to clearly indicate the photoswitch of SBB at these wavelengths.

 ©AUTHOR(S)

While this process is most of the time reversible, we have made our best efforts to identify the necessary conditions to reverse the photoswitch process, by photo or thermal conditions, without success up to now.

These observations indicate that irradiation at higher-energy wavelengths promotes a photochemical transformation of SBB that could be attributed to photoisomerization. SBB strongly absorbs in the red region, but the absence of spectral evolution under red irradiation suggests that this pathway may not lead to the structural modification observed under UV/blue excitation. Therefore, rather than redirecting our strategy solely toward blue or UV irradiation, these results highlight the importance of selecting irradiation conditions that favor productive excited-state pathways while minimizing competing photochemical transformations of the catalyst. With these results in hand, we have decided to step into photocatalysis and to evaluate the capability of SBB to generate reactive oxygen species (ROS) under a range of wavelength irradiation.

ROS generation. Indeed, in photochemical and photodynamic processes, two main pathways lead to the generation of ROS. Two families of ROS can be evaluated, following type I or type II mechanisms. Type I involves electron or hydrogen transfer from the excited photosensitizer to surrounding substrates, producing radical species such as superoxide, hydroxyl radicals, or hydrogen peroxide. In contrast, the type II mechanism relies on energy transfer to ground-state molecular oxygen ($^3O_2$), yielding singlet oxygen ($^1O_2$). The evaluation of ROS generation by SBB was performed directly on chemical transformations driven by these photocatalytic processes, under several irradiation wavelengths (390, 450 and 660 nm, represented as purple, blue and red LEDs on Figure 5). The generation of ROS type II, favored by energy transfer, was evaluated on the oxidation of 1,3-diphenylisobenzofuran (DPBF) [33] (Figure 5, reaction #1) as well as the oxidation of 1,5-dihydroxynaphthalene (1,5-DHN) leading to juglone[34] (Figure 5, reaction #2). On the other hand, the generation of ROS type I, allowed by electron transfer, was evaluated on the hydroxylation of boronic acid into the corresponding alcohol [35] (Figure 5, reaction #3) as well as the oxidation of benzyl alcohol into the corresponding aldehyde [36] (Figure 5, reaction #4). Control experiments have been performed for each reaction (without PC or without light) to ensure the accuracy of the observations made.

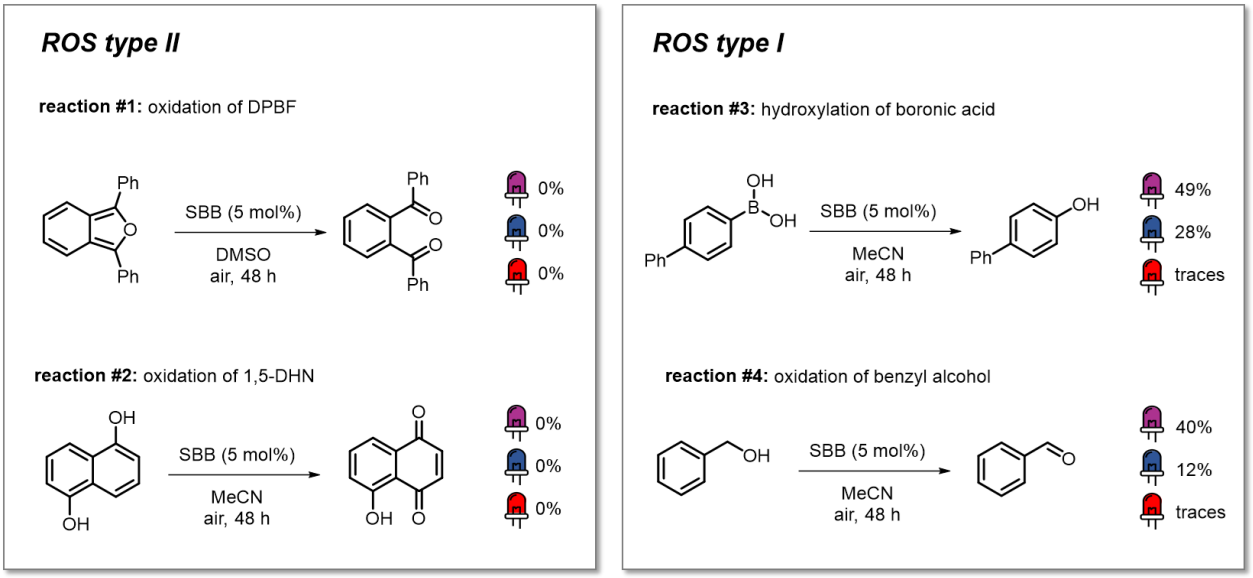

Figure 5. Chemical transformations evaluated with SBB as photocatalyst. Estimated yields were calculated by UPLC-UV-MS.

 ©AUTHOR(S)

Reactions involving ROS type II mechanism, meaning singlet oxygen generation, have shown no conversion, regardless of the wavelength of irradiation. This means that SBB is not able to undergo an energy transfer mechanism from its excited state. However, reactions involving ROS type I generation, most importantly peroxide radical, afforded decent conversions. Indeed, SBB allowed the conversion of boronic acid into the corresponding alcohol with 49% conversion under purple light and 28% conversion under blue light. Similarly, SBB was able to perform the oxidation of benzyl alcohol into the corresponding aldehyde with 40% conversion under purple light and 12% conversion under blue light. Both reactivities suggest that SBB can act as a PC via electron transfer, in reactions involving reactive oxygen species following a type I mechanism. Reactivity of SBB under purple light appears to be more efficient than under blue light, which correlates with the earlier photoswitching observations showing improved switching performance under purple irradiation compared to blue light.

That said, the conversions remain limited. Although a more in-depth analysis of SBB to assess its redox properties would provide a better understanding of the full extent of its potential, it is clear that this structure is unlikely to compete with established photocatalysts such as 4-CzIPN. However, the present evidence that a diazo compound can act as a photocatalyst positions this study as an initial step toward broader exploration of the many azo and diazo compounds already available.

Although this study represents a first step in evaluating commercially available organic dyes as potential photocatalysts, it validates a high-throughput screening methodology that enables the rapid identification of new structures of interest to address current challenges in the field.

Conclusions

In summary, we have investigated the potential of Sudan Black B as an organic photocatalyst identified through high-throughput screening of commercially available dyes. Optical studies revealed strong visible-light absorption, pronounced solvent-dependent spectral shifts, and photoinduced structural changes under UV and blue irradiation, consistent with azo photoswitching behavior. Photocatalytic experiments demonstrated that SBB is capable of promoting oxidative transformations through a reactive oxygen species pathway consistent with a Type I electron-transfer mechanism, while no significant singlet oxygen generation was detected. Given the vast structural diversity of azo and diazo compounds already accessible on the market, this approach opens new opportunities for rapidly expanding the toolbox of sustainable and economically viable organic photocatalysts.

Experimental Section

General. Unless otherwise noted, all reactions were carried out in oven-dried glassware. Commercially available chemicals were purchased from ABCR, Acros Organics, Sigma-Aldrich, Alfa Aesar, Combi-Blocks, Carbolution, Fluorochem, BLD Pharm and TCI Europe and used as received unless otherwise stated. The following solvents were dried by distillation over the drying agents indicated in parentheses: THF (Sodium) and dichloromethane (CaH2). Additional anhydrous solvents were purchased from Acros Organics, SigmaAldrich, Alfa Aesar and stored over molecular sieves under an argon atmosphere.

LC-MS spectra were recorded on a Waters Acquity UPLC® equipped PDA eλ Detector and SQ Detector 2, mobile phase A: H2O + 0.1% formic acid, mobile phase B: acetonitrile + 0.1% formic acid.

 ©AUTHOR(S)

For HTE campaign, the HTE facility of the CEA Paris Saclay has been used. For HTE analysis the following analytical method was used: Run length 8 min; column type: ACQUITY UPLC® CSH™ Phenyl-Hexyl 1.7 µm.

General procedure for photocatalyzed hydroxylation of boronic acid. (4'-methoxy-[1,1'-biphenyl]-4-yl)boronic acid (1 equiv.) and SBB (5 mol%) were added to an 8 mL vial equipped with a stir bar. DMF (0.1 M) and DIPEA (2 equiv.) were added. The reaction mixture (open to air) was stirred for 48 h under 660 nm irradiation. Estimated conversion (HPLC) =
under UV light: 48.78%;
under blue light: 27.70%;
under red light: 0%.
General procedure for the photocatalyzed oxidation of benzyl alcohol. Benzyl alcohol (1 equiv.) and SBB (5 mol%) were added in an 8 mL vial equipped with a stir bar. Then DMSO (0.1M) was added, the reaction was kept under air and the vial was closed with a cap. The reaction mixture was stirred for 48 h under irradiation.
Estimated conversion (HPLC)=
under UV light: 40.20%;
under blue light: 11.68%;
under red light: 3.96%.

Acknowledgements

All authors thank the CEA for the PhD funding of Marine Le Stum via a CFR grant. All authors thank S. Lebrequier, T. D'Anfray and D. Buisson for the development of analytical methods and fruitful discussions. All authors also warmly thank the technical support of the SCBM.

Supplementary Material

Details on the HTE campaign, optical studies and chemical transformations performed are available in the supplementary material file associated with this paper.

References

1. Prier, C. K.; Rankic, D. A.; MacMillan, D. W. C. *Chem. Rev*. **2013**, *113*, 5322–5363. https://doi.org/10.1021/cr300503r
2. Shaw, M. H.; Twilton, J.; MacMillan, D. W. C. *J. Org. Chem*. **2016**, *81*, 6898–6926. https://doi.org/10.1021/acs.joc.6b01449
3. Romero, N. A.; Nicewicz, D. A. *Chem. Rev*. **2016**, *116*, 10075-10166. https://doi:10.1021/acs.chemrev.6b00057
4. Capaldo, L.; Ravelli, D. *Eur. J. Org. Chem*. **2020**, *2020*, 19, 2783-2806. https://doi.org/10.1002/ejoc.202000144
5. Arias-Rotondo, D. M.; McCusker, J. K. *Chem. Soc. Rev*. **2016**, *45*, 5803-5820. https://doi.org/10.1039/c6cs00526h

 ©AUTHOR(S)

6. Gkizis, P. L. *Eur. J. Org. Chem*. **2022**, e202201139. https://doi.org/10.1002/ejoc.202201139
7. Demertzidou, V. P.; Skolia, E.; Kokotos, C. G. *ChemCatChem* **2025**, *16*, e00760. https://doi.org/10.1002/cctc.202500760
8. Li, P.; Terrett, J. A.; Zbieg, J. R. *ACS Med. Chem. Lett.* **2020**, *11*, 2120-2130. https://doi.org/10.1021/acsmedchemlett.0c00436
9. Callard-Langdon, E. E.; Steven, A.; Kahan, R. J. *ChemCatChem* **2023**, 15, e202300537. https://doi.org/10.1002/cctc.202300537
10. Vos, J. G.; Kelly, J. M. *Dalton Trans*. **2006**, 4869-4883. https://doi.org/10.1039/b606490f
11. Marin, V.; Holder, E.; Hoogenboom, R.; Schubert, U. S. *Chem. Soc. Rev*. **2007**, *36*, 618-635. https://doi.org/10.1039/b610016c
12. Daniel, C. *Coord. Chem. Rev*. **2015**, *282283*, 19-32. https://doi.org/10.1016/j.ccr.2014.05.023
13. Fantacci, S.; De Angelis, F. *Coord. Chem. Rev.* **2011**, *255*, 2704–2726. https://doi.org/10.1016/j.ccr.2011.03.008
14. Paris, J. P.; Brandt, W. W. *J. Am. Chem. Soc.* **1959**, *81*, 5001–5002. https://doi.org/10.1021/ja01527a064
15. Lowry, M. S.; Goldsmith, J. I.; Slinker, J. D.; Rohl, R.; Pascal, R. A.; Malliaras, G. G.; Bernhard, S. *Chem. Mater.* **2005**, *17*, 5712–5719. https://doi.org/10.1021/cm051312+
16. Shang, T. Y.; Lu, L. H.; Cao, Z.; Liu, Y.; He, W. M.; Yu, B. *Chem. Commun.* **2019**, *55*, 5408–5419. https://doi.org/10.1039/c9cc01047e
17. Nicewicz, D. A.; Nguyen, T. M. *ACS Catal.* **2014**, *4*, 355–360. https://doi.org/10.1021/cs400956a
18. Ravelli, D.; Fagnoni, M. *ChemCatChem* **2012**, *4*, 169–171. https://doi.org/10.1002/cctc.201100363
19. Ravelli, D.; Fagnoni, M.; Albini, A. *Chem. Soc. Rev.* **2013**, *42*, 97–113. https://doi.org/10.1039/c2cs35250h
20. Benkhaya, S.; M'Rabet, S.; El Harfi, A. *Heliyon* **2020**, *6*, e03271. https://doi.org/10.1016/j.heliyon.2020.e03271
21. Chang, V. Y.; Fedele, C.; Priimagi, A.; Shishido, A.; Barrett, C. J. *Adv. Opt. Mater.* **2019**, *7*, 1900091. https://doi.org/10.1002/adom.201900091
22. Wang, T.; Sun, W.; Zhang, X.; Xu, H.; Xu, F. *Materials* **2017**, *10*, 1247. https://doi.org/10.3390/ma10111247
23. https://microbenotes.com/sudan-black-b-staining/
24. Giatromanolaki, A.; Kouroupi, M.; Balaska, K.; Koukourakis, M. I. *Pathol. Res. Pract.* **2020**, *216*, 152800. https://doi.org/10.1016/j.prp.2019.152800
25. Iwata, H.; Kami, M.; Kishi, Y.; et al. *Leukemia* **2000**, *14*, 2013–2014. https://doi.org/10.1038/sj.leu.2401927
26. Krska, S. W.; DiRocco, D. A.; Dreher, S. D.; Shevlin, M. *Acc. Chem. Res.* **2017**, *50*, 2976–2985. https://doi.org/10.1021/acs.accounts.7b00428
27. Schmink, J. R.; Bellomo, A.; Berritt, S. *Aldrichim. Acta* **2013**, *46*, 71–80. http://www.sigmaaldrich.com/content/dam/sigma-aldrich/docs/Aldrich/Brochure/1/acta-46-3.pdf

 ©AUTHOR(S)

28. Isbrandt, E. S.; Sullivan, R. J.; Newman, S. G. *Angew. Chem. Int. Ed.* **2019**, *58*, 7180–7191. https://doi.org/10.1002/anie.201812534
29. Shevlin, M. *ACS Med. Chem. Lett.* **2017**, *8*, 601–607. https://doi.org/10.1021/acsmedchemlett.7b00165
30. Allen, C. L.; Leitch, D. C.; Anson, M. S.; Zajac, M. A. *Nat. Catal.* **2019**, *2*, 2–4. https://doi.org/10.1038/s41929-018-0220-4
31. Caldentey, X.; Romero, E. *Chem. Methods* **2023**, *3*, e202200059. https://doi.org/10.1002/cmtd.202200059
32. Zakerhamidi, M. S.; Seyed Ahmadian, S. M.; Kian, R. *Can. J. Chem.* **2015**, *93*, 639-647. https://doi.org/10.1139/cjc-2014-0489
33. Öztürk Gündüz, E.; Büyükpolat, Ü.; Okutan, E. *J. Fluoresc.* **2025**, *11*, 11651–11662. https://doi.org/10.1007/s10895-025-04391-y
34. Takizawa, S.-Y.; Aboshi, R.; Murata, S. *Photochem. Photobiol. Sci.* **2011**, *6*, 895–903. https://doi.org/10.1039/C0PP00265H
35. Yang, H.-M.; Liu, M.-L.; Tu, J.-W.; Miura-Stempel, E.; Campbell, M. G.; Chuang, G. *J. Org. Chem.* **2020**, *4,* 2040–2047. https://doi.org/10.1021/acs.joc.9b02777
36. Chiang, C.-W.; Chou, Y.-H.; Chou, C.-H.; Chen, H.-C.; Chen, J.-L.; Hsu, L.-C.; Huang, W.-H.; Li, H.-L.; Liu, Y.-H. *Eur. J. Inorg. Chem*. **2024**, *3*, e202300516. https://doi.org/10.1002/ejic.202300516

This paper is an open access article distributed under the terms of the Creative Commons Attribution (CC BY) license (http://creativecommons.org/licenses/by/4.0/)